

# STORAGELESS RESONANT CONVERTER FOR ACCELERATOR MAGNETS

M. Cautero, T. N. Gučin, Elettra Sincrotrone Trieste, Trieste, Italy

## Abstract

Elettra Sincrotrone Trieste, a specialized research centre generating high quality synchrotron radiation, has been in operation since 1993 and was revised in 2009. Recently, Elettra has been funded for a complete renewal of the storage ring. For the new machine, it is planned to employ state of the art converters, mostly of which will be designed in-house.

For this purpose, it has been decided to evaluate the performance of a storage-less resonant converter, proposed by Dr. Slobodan Čuk, which is a step down DC/DC converter consisting of four switches, one resonant capacitor and two resonant inductors. For this purpose, the voltage conversion ratio of the converter has been derived. The topology was confirmed with simulation and a PCB layout has been designed, which is still to be tested.

## ELETTRA SINCROTRONE TRIESTE

Low current magnets have been designed for the new 6BA design of the storage ring, so that each one will be independently energized. With a larger number of power supplies, the main goal is to get high efficiency to keep the facility environmentally friendly and rise the MTBF by lowering the thermal stresses on active devices. The following converter is fulfilling our two requirements.

## STORAGELESS RESONANT CONVERTER

The examined storage-less resonant converter proposed by Dr. Slobodan Čuk [1], illustrated in Fig. 1.a, mainly relies on the energy transfer by resonance, instead of storing energy in inductors such as in buck converters.

As it can be seen in Fig. 1, the converter is composed of four switches ( $Q_1$  to  $Q_4$ ), two resonance inductors ( $L_{r1}$  and  $L_{r2}$ ), one resonant capacitor ( $C_r$ ) and one output filter capacitor ( $C_o$ ).

The basic operation principle of this converter is to charge the resonant capacitor ( $C_r$ ) by means of a resonance circuit formed with one of the inductors and to discharge the same capacitor through the other resonant inductor. This way, the transferred energy does not need to be stored in an inductive element, such as the case of a buck converter.

Although the structure is similar to switched capacitor converters [2], the addition of resonant inductances changes the operation of the converter and requires two of the switches, namely  $Q_3$  and  $Q_4$ , to operate like diodes. This also in return, enables the converter to operate at higher efficiencies for a wider range.

## Basic Operation Principle

The operation principle of the converter will be explained over the simplest case, where resonance inductors have the same value,  $L_{r1} = L_{r2}$ , switching frequency is equal to the resonance frequency,  $f_r$ , and the duty cycle,  $D$ , is equal to 50%. Here  $D$  is defined as

$$D = T_1 \cdot f_r \quad (1)$$

Where  $T_1$  is the time interval where the switches  $Q_1$  and  $Q_3$  are conducting.

As it can be seen in Fig. 1.a and Fig. 1.b, there are two main operational states of the converter. In the first state, the resonant capacitor,  $C_r$ , is charged through the switches  $Q_1$  &  $Q_3$  and  $L_{r1}$ . In this state, the current is supplied by the input voltage source and  $C_r$  is being charged.

In the second state, the switches  $Q_1$  &  $Q_3$  are turned off, while the switches  $Q_2$  and  $Q_4$  are turned on. In this state, the power for the load is provided by the resonant capacitor, which is being discharged. As seen above, the switch pairs  $Q_{1,3}$  and  $Q_{2,4}$  are operated complementary to each other.

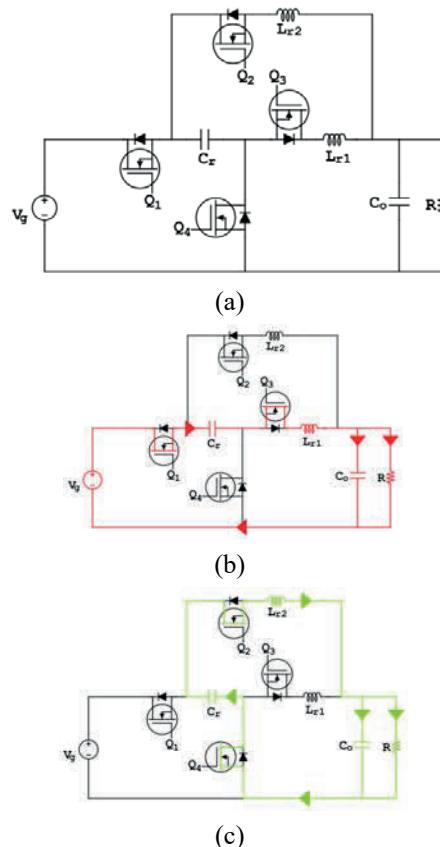


Figure 1: (a) Storage-less Resonant Converter and operation intervals of the converter; while (a) resonant capacitor is charging and (b) is discharging.

Content from this work may be used under the terms of the CC BY 3.0 licence (© 2019). Any distribution of this work must maintain attribution to the author(s), title of the work, publisher, and DOI

For mentioned states, the following voltage equations can be written, which are basically second order ordinary differential equations:

$$V_g - V_o = V_{cr} + V_{Lr1} = \frac{1}{C_r} \int i_{Lr1} dt + L_{r1} \frac{di_{Lr1}}{dt} \quad (2)$$

$$V_o = V_{cr} - V_{Lr2} = \frac{1}{C_r} \int i_{Lr2} dt - L_{r2} \frac{di_{Lr2}}{dt} \quad (3)$$

The solutions for these equations are sinusoidal waveforms, which are as follows:

$$i_{Lr1}(t) = \frac{(V_g - V_o)}{\sqrt{L_{r1}/C_r}} \cdot \sin(\omega_1 t) \quad (4)$$

$$i_{Lr2}(t) = \frac{V_o}{\sqrt{L_{r2}/C_r}} \cdot \sin(\omega_2 t) \quad (5)$$

Where,

$$\omega_1 = \frac{1}{\sqrt{L_{r1} \cdot C_r}} \quad (6)$$

$$\omega_2 = \frac{1}{\sqrt{L_{r2} \cdot C_r}} \quad (7)$$

The current waveforms on the resonant inductors are illustrated in Fig. 2. As it can be seen, the current waveforms are sinusoidal and the magnitudes of the currents at switching instances are equal to zero, which enables soft switching Zero Current Switching (ZCS) for all four switches.

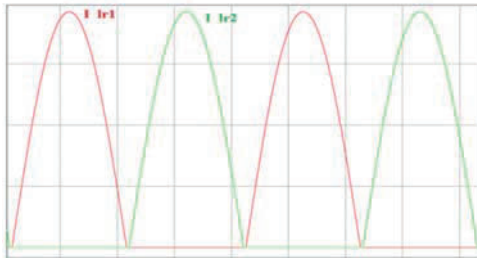


Figure 2: Resonant inductor current waveforms at D = 0.5.

The voltage conversion ratio at this case can be calculated considering the fact that the total change of the capacitor charge during one cycle at steady state should be zero. If the Equations (4) and (5) are integrated and equated, it will be seen that:

$$V_o = V_g - V_o \quad (8)$$

$$V_o = \frac{V_g}{2} \quad (9)$$

Where,  $V_g$  is input voltage and  $V_o$  is output voltage. This is the maximum achievable output voltage for this converter.

### Constant Off-Time Variable On-Time Control

The operation of the converter can be extended to duty cycles that are different than 50%, which in return governs the output voltage.

However, it is obvious that if the switches are turned on/off with a period different than the resonant frequency, the ZCS feature will not be achieved anymore. Thus, the efficiency will decrease.

For maintaining the ZCS feature as much as possible, it is better to use a constant off-time and variable on-time control strategy, where the on time of the switches  $Q_2$  and  $Q_4$  are fixed to be equal to the half of the second resonance period  $T_2$  and the on-time of switches  $Q_1$  and  $Q_3$  are varied.

$$T_2 = 2 \cdot \pi / \omega_2 \quad (10)$$

This way, the switches  $Q_2$  and  $Q_4$  always operate at ZCS turn-on and ZCS turn-off. Moreover, it is also obvious that for preventing any abrupt change of current on  $L_{r1}$ , the  $Q_3$  has to behave like a diode. Thus, it has been connected in a reverse way, so that the body diode will always ensure diode operation. The current waveforms for this operation are shown in Fig. 3.

Utilizing the constant-off time strategy, switches  $Q_1$  and  $Q_3$  still maintain the ZCS turn-on operation, whereas the switch  $Q_1$  has to turn off while it is conducting a high amount of current.

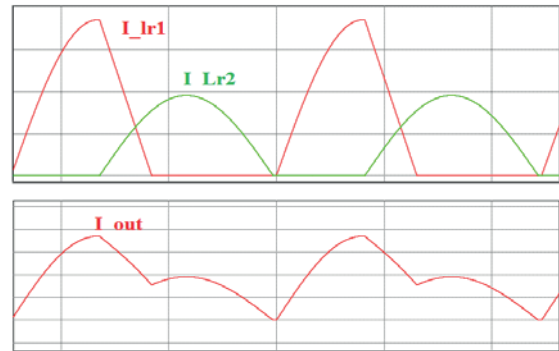


Figure 3: Resonant inductor current waveforms at D = 0.5.

The analysis of the converter under constant off-time control results in the following polynomial equation as the expression of output voltage:

$$V_o^2 \left[ 4 \cdot K - \frac{4 \cdot A \cdot C_r}{\left(1 - \frac{A}{2}\right)} - \frac{T_{sw}}{R} \right] + V_o \left[ \frac{2 \cdot A \cdot C_r \cdot V_g}{\left(1 - \frac{A}{2}\right)} - 4 \cdot V_g \cdot K \right] + V_g^2 \cdot K \quad (11)$$

Where  $T_{sw} = T_1 + T_2/2$  is the switching period,

$$K = \left( \frac{\sin(\omega_1 T_1)}{\left(1 - A/2\right)} \right)^2 \cdot \frac{C_r \cdot L_{r2}}{2 \cdot L_{r1}} \quad (12)$$

$$A = \left(1 - \cos(\omega_1 T_1)\right) \quad (13)$$

The solution of the quadratic polynomial function for the case of  $L_{r1}=L_{r2}$  (meaning  $f_1=f_2=f_r$ ), at various loads are illustrated in Fig. 4. As given previously, here the duty cycle is  $D=T_1 \cdot f_r$ , and normalized output voltage is  $V_{on} = V_o/V_g$ .

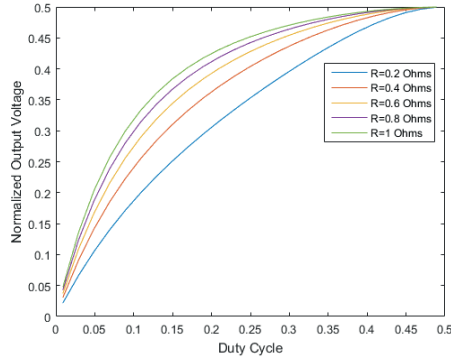


Figure 4: Resonant inductor current waveforms at  $D = 0.5$ .

### SIMULATIONS

According to the parameters in Table 1, a simulation model, shown in Fig. 5, has been built via PSIM 11, for checking the behaviour of the converter.

To ensure low current ripple at the input and output, it has been decided to employ an LC filter at the input and Pi filter at the output.

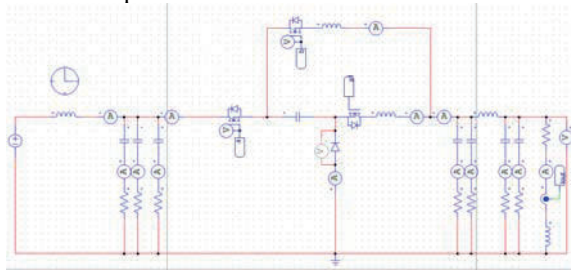


Figure 5: Simulation model in PSIM 11.

Table 1: Designed Circuit Parameters

Parameter	Value
Input Voltage, $V_g$	48 Volts
Max. Output Voltage, $V_{out}$	24 Volts
Max. Output Current, $I_{out}$	60 Amperes
Resonance Frequency, $f_{res}$	159 kHz
Resonant Capacitor, $C_r$	5 $\mu$ F
Resonant Inductor 1, $L_{r1}$	200 nH
Resonant Inductor 2, $L_{r1}$	200 nH
GaN FETs	EPC2020
Gate Driver	Si8274
Synch. Rect. Controller	UCC24612-1

### PCB DESIGN

The chosen GaNFET is particularly small and adds some manufacturing issues for the width of the pads (270  $\mu$ m) which are replicated on all 8 layers of 35  $\mu$ m thickness PCB, shown in Fig. 6. Vias with the hole of 100  $\mu$ m are needed on the pads to split the current (60 Amps) flowing

on the drains of the transistors. The overall size of this converter is 165 x 75 mm (including the 30 mm gap for current probe) for a 1400 W device. Two of the GaNFETs are controlled with synchronous rectifier controllers so that they work like diodes. Thermal losses are predicted to be maximum 30 W.

The PCB has been employed with multi-layer ceramic capacitors only for size shrinking. The used inductors are quite small, since they are only 200 nH.

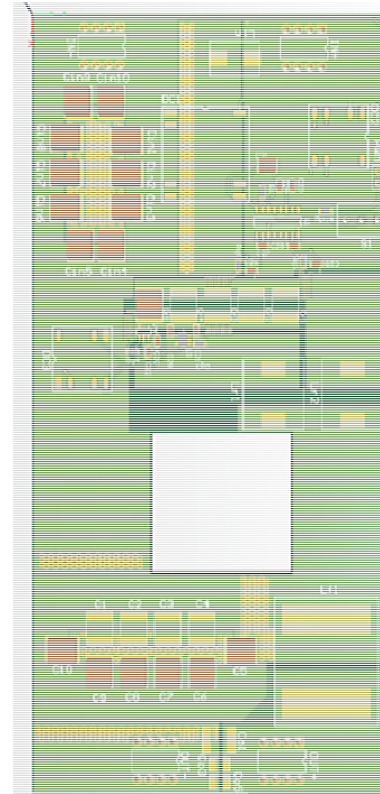


Figure 6: Designed PCB layout.

### CONCLUSION

At the present time the PCB has been designed and manufactured and needs mounting the GaNFETs. Results from the field will be made available.

The clear advantage of the examined topology is the usage of very small inductances without the need for increasing the switching frequency to MHz levels. This is due to the fact that the energy transfer relies on resonance. Moreover, three of the GaNFETs are operated in soft switching mode, whereas only one is operating at hard turn-on.

### REFERENCES

- [1] S. Čuk, "Four-Switch Step-down Storageless Converter", United States Patent US 8, 134, 351 B2, Mar. 13, 2012.
- [2] A. Cervera *et al.*, "A High-Efficiency Resonant Switched Capacitor Converter With Continuous Conversion Ratio", *IEEE Transactions on Power Electronics*, vol. 30, no. 3, pp. 1373-1382, Mar. 2015.

Content from this work may be used under the terms of the CC BY 3.0 licence (© 2019). Any distribution of this work must maintain attribution to the author(s), title of the work, publisher, and DOI